

## Theoretical study of the stabilization mechanisms of the different stable oxygen incorporated (10 $\bar{1}$ 0) surface of III-nitrides

Honggang Ye,<sup>a)</sup> Guangde Chen, Yelong Wu, and Youzhang Zhu  
 MOE Key Laboratory for Nonequilibrium Synthesis and Modulation of Condensed Matter,  
 School of Science, Xi'an Jiaotong University, Xi'an 710049, People's Republic of China

(Received 13 October 2009; accepted 17 January 2010; published online 25 February 2010)

By using the first-principles calculation methods, the stable structures of oxygen incorporated (10 $\bar{1}$ 0) surface of AlN and InN are explored in comparison with that of GaN. The one for AlN is found to be  $V_{\text{Al}}-(\text{O}_{\text{N}})_3$ , a complex of Al vacancy and three substitutional O in N sites, while the one for InN is consistent with that of GaN, which is comprised by two monolayers of O replacing the N atoms, denoted by  $2(\text{O}_{\text{N}})$ . The stabilization mechanisms of the two surface structures and the origin of the discrepancy between AlN and GaN are further given by analyzing their electronic structures. © 2010 American Institute of Physics. [doi:10.1063/1.3311557]

Group-III nitrides are of great interest for microelectronic and optoelectronic applications. Attention to them has expanded from GaN to AlN and InN binary compounds. AlN possesses a large band gap, high thermal conductivity, small thermal expansion coefficient, and high electrical resistivity.<sup>1–3</sup> It can be used for UV emitters, lasers, and high-mobility transistors, and also can be used as a substrate or buffer layer for the growth of group-III nitrides and their alloys.<sup>4,5</sup> The outstanding property of InN is the small effective mass, which leads to a large electron mobility and a high carrier saturation velocity.<sup>6,7</sup> Thus, it is a good candidate for high-performance heterojunction field-effect transistors.

Interest in the nonpolar wurtzite (10 $\bar{1}$ 0) surface of III-nitrides arises for several reasons. First, the stoichiometric surface is expected to form in the process of fracture because it is stable over a wide range of conditions. Second, the epitaxial films grown along the [10 $\bar{1}$ 0] direction can decrease or eliminate the large polarization field in the polar films.<sup>8,9</sup> Increasing efforts have been done to the growth of the nonpolar films. Detailed studies of the structure and property of the (10 $\bar{1}$ 0) surface are therefore needed to the improvement of film quality and further applications. Finally, the (10 $\bar{1}$ 0) surface often presents as the main component of the lateral facets of the nanowires and nanotubes.<sup>10,11</sup> Surface property study is important to understand the features of these nanostructures.

Oxygen is usually one of the unintended impurities incorporated in crystal lattice or adsorbed at the surfaces of III-nitrides. In the case of GaN, much attention has been attracted by the oxygen incorporated (10 $\bar{1}$ 0) surface because it was found to be responsible for the formation of some extended defects, such as dislocations and nanopipes, which are generally observed in GaN epitaxial films.<sup>12–15</sup> Elsner *et al.*<sup>16</sup> suggested that a complex consisting of a Ga vacancy and three substitutional O atoms at surrounding N sites, called  $V_{\text{Ga}}-(\text{O}_{\text{N}})_3$ , is energetically stable by density func-

tional theory (DFT) calculation, while theoretical work of Northrup *et al.*<sup>17</sup> reveals that a structure with substitutional O in N-sites of the top two layers, named  $2(\text{O}_{\text{N}})$ , is more stable. However, the intrinsic stabilization mechanism of  $2(\text{O}_{\text{N}})$  has not been clearly explored.

The ideal (10 $\bar{1}$ 0) surface of GaN introduces an occupied surface state above the valance-band-maximum (VBM) and an empty surface state below the conduction-band-minimum (CBM), which are usually designated by  $B_5$  and  $C_3$ , respectively. In general, as reported in Ref. 16, the  $V_{\text{Ga}}-(\text{O}_{\text{N}})_3$  is thought to be more stable than the  $2(\text{O}_{\text{N}})$  because the additional electrons introduced by O atoms in the  $2(\text{O}_{\text{N}})$  structure occupy the high  $C_3$  band, which therefore induces a high energy, but the Ga vacancy in the  $V_{\text{Ga}}-(\text{O}_{\text{N}})_3$ , which acts as a triple acceptor, can empty the  $C_3$  band and therefore induces a low energy. The truth for GaN, however, is opposite with the empirical predication. The origin of this abnormal phenomenon is explored in the present work by analyzing their electronic band structures.

In contrast with GaN, theoretical works have not yet been seen in literatures about the interaction of oxygen with the nonpolar (10 $\bar{1}$ 0) surfaces of wurtzite AlN and InN. So the structures of the oxygen incorporated (10 $\bar{1}$ 0) surfaces of AlN and InN are investigated in this work by first-principles calculation methods. The above two structures are still mainly considered because they are the most possible candidates. The III-nitrides may be thought to have the same stable oxygen incorporated surface structures because of their similarities, but the truth is unexpected. The one for InN is the same as that for GaN but the one for AlN is the  $V_{\text{Al}}-(\text{O}_{\text{N}})_3$ , which is opposite to that of GaN. The origin of this interesting discrepancy is also discussed in this paper.

The DFT calculations in this work are performed within the generalized gradient approximation<sup>18</sup> framework as implemented by the Vienna *Ab initio* Simulation Package code.<sup>19,20</sup> We employ Vanderbilt ultrasoft pseudopotentials.<sup>21</sup> The energy cutoff for the plane wave basis function is 500 eV for AlN and 700 eV for GaN and InN. We employ the Monkhorst–Pack sampling scheme with a density of  $5 \times 8$

<sup>a)</sup>Electronic mail: yehonggang@stu.xjtu.edu.cn.

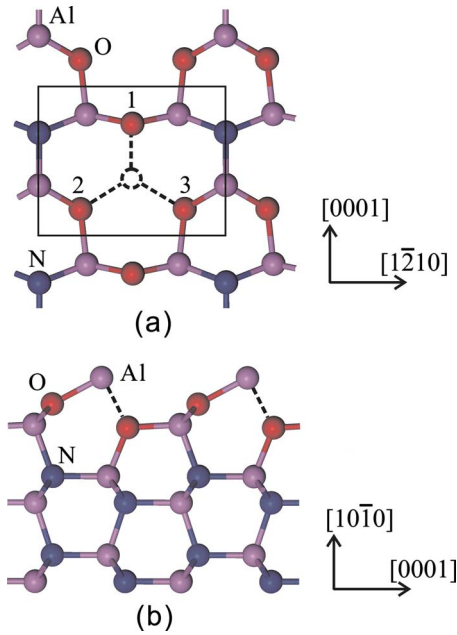


FIG. 1. (Color online) Schematic representations of (a) top view of the relaxed  $V_X-(O_N)_3$  ( $X=\text{Al, Ga, and In}$ ) and (b) side view of the relaxed  $2(O_N)$ .

$\times 1$  k-point mesh for the  $(1 \times 1)$   $(10\bar{1}0)$  surface.<sup>22</sup> The slab models are built containing 16 atomic layers with 12 Å vacuum space separating the slabs. The top four layers at each side of the slabs are allowed to relax by minimizing the quantum mechanical force on each ion to be less than 0.01 eV/Å. The other layers are fixed in the optimized bulk configuration. Test calculations show that the cell size is converged, and the consistency between the results of Northrup *et al.*<sup>17</sup> and ours for GaN is also a validation of our calculations.

Top view of the relaxed  $V_X-(O_N)_3$  ( $X=\text{Al, Ga, In}$ ) is schematically represented in Fig. 1(a). The black rectangle exhibits a unit cell, which is a  $(2 \times 1)$  cell including a  $V_X-(O_N)_3$  complex and a  $XN$  dimer. The position of the removed cation is shown by the dashed circle. The O atom denoted by 1 is in the first atomic layer and is two coordinated. The other two ones denoted by 2 and 3 are in the second atomic layer and are three coordinated. Side view of the relaxed  $2(O_N)$  is schematically shown in Fig. 1(b). The surface O atoms tend to move inward, and the surface cations tend to move outward after relaxation. The two back bonds of top layer cation, shown by the dashed lines, have been elongated by about 30%, thus become very weak. The interest is that this relaxation model is contrary to that of the ideal  $(10\bar{1}0)$  surface of III-nitrides,<sup>23,24</sup> in which the surface cations shift inward but anions shift outward. That is because the additional electrons introduced by substitutional O atoms are accepted by the cation dangling bond. Repulsion between the bonds makes it occur.

The formation energies of the considered models are shown in Fig. 2. The details of the calculation are described below by taking AlN as an example. The atomic chemical potential of Al is restricted in the thermodynamically allowed range of  $\Delta H_{\text{AlN}} < \mu_{\text{Al}} - \mu_{\text{Al}(\text{bulk})} < 0$ , where  $\mu_{\text{Al}}$  and

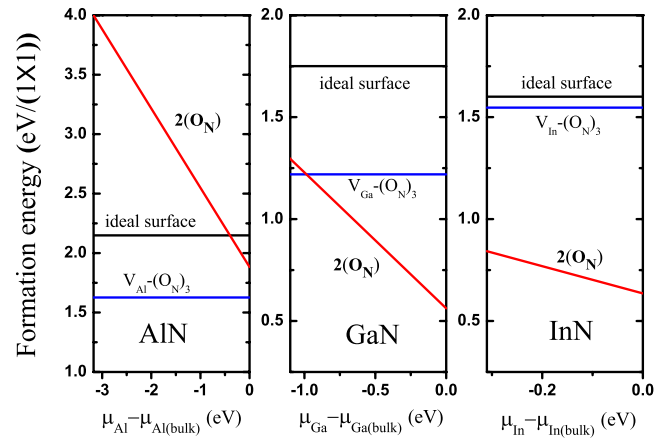


FIG. 2. (Color online) Formation energies of the oxygen incorporated  $(10\bar{1}0)$  surface models as a function of the cation chemical potential.

$\mu_{\text{Al}(\text{bulk})}$  are the free and bulk Al chemical potentials, respectively, and  $\Delta H_{\text{AlN}}$  is the formation enthalpy of bulk AlN. The chemical potentials of N and O are derived from the equations of  $\mu_{\text{Al}} + \mu_{\text{N}} = E_{\text{AlN}}$  and  $2\mu_{\text{Al}} + 3\mu_{\text{O}} = E_{\text{Al}_2\text{O}_3}$ , respectively, in which  $E_{\text{AlN}}$  and  $E_{\text{Al}_2\text{O}_3}$  are the total energy of bulk AlN and  $\alpha\text{-Al}_2\text{O}_3$ . It can be seen from Fig. 2 that the  $V_{\text{Al}}-(O_N)_3$  is with the lowest formation energy in the whole range of the possible Al chemical potential, while the stable structure is the  $2(O_N)$  for GaN and InN. We neglect the small exception for GaN in the very N-rich condition, where the  $V_{\text{Ga}}-(O_N)_3$  is more stable, because the calculated range of the chemical potential is usually not very consistent. The range for Ga is 1.1 eV here but 0.9 eV in Ref. 17, where this exception does not exist. It is obvious that the AlN  $(10\bar{1}0)$  surface possesses a different stable oxygen incorporated surface structure with respect to GaN and InN. The common ground for the three binaries is that the formation energies of the stable oxygen incorporated surfaces are lower than that of the ideal surfaces, which indicates that they are easy to be oxidized.

To understand the stabilization mechanism of the  $2(O_N)$  for GaN, its electronic band structure is computed and revealed in Fig. 3(a). The green (triangular) line is a fully occupied band, which has nearly touched the VBM at the  $\Gamma$  point. It is, in fact, the  $C_3$  band of the clean GaN  $(10\bar{1}0)$  surface, which is originally an empty band lying closely below the CBM. The considerable downward shift of this band is from the surface relaxation induced by the additional electrons of the O atoms. This action must be associated with the reduction in formation energy but it is neglected in the previous empirical predication. So we can conclude that the  $2(O_N)$  is stabilized by the downward shift of the filled  $C_3$  band. The blue (quadrilateral) line present in the upper part of the band gap is from the elongation of the two back bonds of the surface Ga. It is an empty state and therefore has no effect on energy.

The electronic band structure of the  $2(O_N)$  for AlN is shown in Fig. 3(b). The downward shift of the  $C_3$  band also occurs, but why is the  $2(O_N)$  not stable for AlN? It can be partially attributed to the large band gap and the wide dispersion of the  $C_3$  band of AlN, which makes the Fermi level

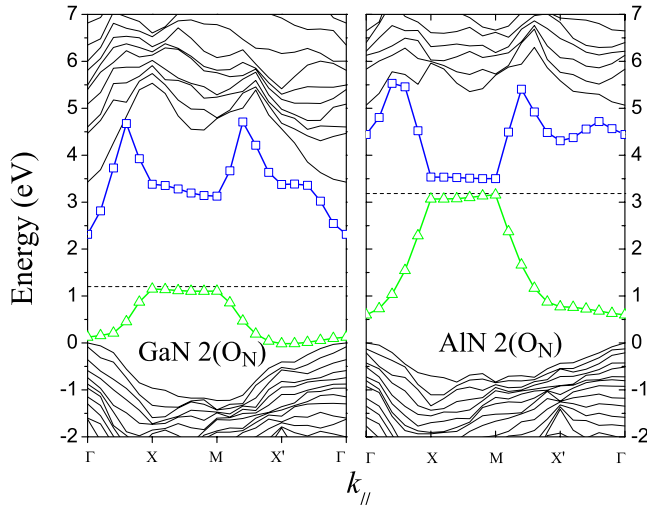


FIG. 3. (Color online) Electronic band structures of the  $2(O_N)$  for GaN (left) and AlN (right). The horizontal dashed lines present the position of the Fermi level.

high in the band gap, about 3.2 eV above the VBM in contrast with 1.2 eV for GaN. It indicates that the reduction of energy induced by the downward shift of the filled  $C_3$  band is weak for AlN. On the other hand, we should also consider the electronic structures of the  $V_X-(O_N)_3$ . The calculated electronic band structures of the  $V_X-(O_N)_3$  for AlN and GaN are revealed in Figs. 4(a) and 4(b) respectively. The bands in the blue and green lines are the  $B_5$  and  $C_3$  bands, respectively, which originate from the dangling bonds of the XN dimer beside the  $V_X-(O_N)_3$ . The two bands in the red lines are related to the  $V_X-(O_N)_3$ . The Ga(Al) vacancy can introduce three empty states above the VBM. The empty states appear as an empty band and a half occupied band, so there

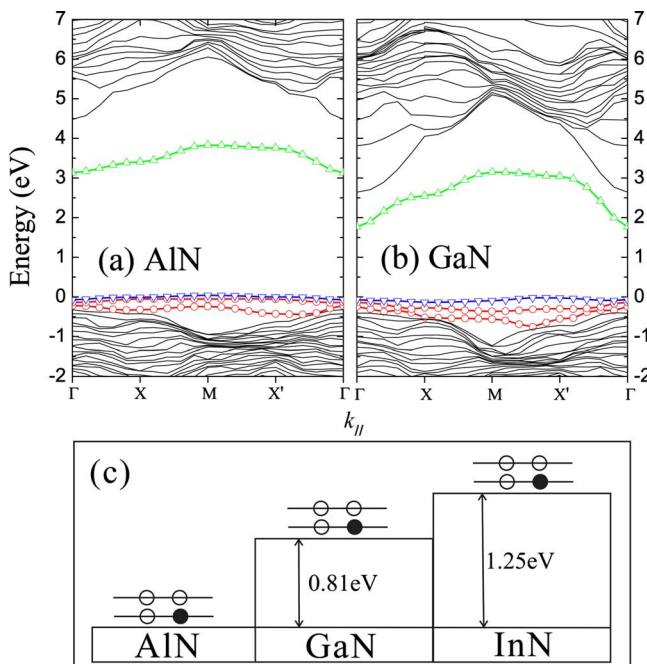


FIG. 4. (Color online) The electronic structures of the  $V_X-(O_N)_3$  structure for (a) AlN and (b) GaN, in which the energy zero is set at the position of the Fermi level. Part (c) is a schematic representation of the valence band offset between AlN, GaN, and InN.

are two bands related to the complex. The three empty states are just fully occupied by the additional electrons of the surrounding O atoms; the obtained two bands thus are below the Fermi level. What we are interested in is that the positions of the two bands relative to the VBM for GaN and AlN are very similar. It does not indicate that their effects on the surface formation energy are equivalent for GaN and AlN, because there is a large valence band offset between them. As shown in Fig. 4(c), the VBM of GaN is higher than that of AlN and the well accepted value of the step is 0.81 eV.<sup>25</sup> Three electrons will create a considerable energy difference. The VBM of InN is 1.25 eV higher than that of AlN. This factor thus is more important for InN.

The result that the AlN  $(10\bar{1}0)$  surface possesses a different stable oxygen incorporated structure with respect to GaN and InN, in fact, is not hard to accept. In our previous works, a stoichiometric planar-defect  $(10\bar{1}0)$  surface was found to be more stable than the ideal surface for AlN, but not for GaN and InN.<sup>26</sup> The adsorption of oxygen on AlN polar  $(0001)$  and  $(000\bar{1})$  surfaces also exhibit different features from GaN.<sup>27</sup> In addition, the crystal-field induced split of the VBM was found to be large and negative for AlN but positive for both GaN and InN.<sup>25</sup> These discrepancies are related to the intrinsic properties of AlN, which include the strong ionicity, the small  $c/a$  (lattice constant ratio), and the lack of cation  $d$  electrons.

In summary, the geometric and electronic structures of the oxygen incorporated  $(10\bar{1}0)$  surfaces of group-III nitrides are investigated by first-principles calculation methods. The complex called  $V_{Al}-(O_N)_3$  is energetically stable for AlN but the stable surface structure for GaN and InN is the  $2(O_N)$ . The stabilization mechanism of the  $2(O_N)$  is attributed to the obvious downward shift of the filled  $C_3$  band. The discrepancy between AlN and GaN is partially from the weak downward shift of the  $C_3$  band of AlN and partially from their large valence band offset.

The authors gratefully acknowledge the financial support of China National Natural Science Fund (Grant No. 10474078) and the computing support of the "Intelligent Information Processing and Computing Lab" of XJTU.

<sup>1</sup>R. R. Lee, *J. Am. Ceram. Soc.* **74**, 2242 (1991).

<sup>2</sup>S. Figge, H. Kroncke, D. Hommel, and B. M. Epelbaum, *Appl. Phys. Lett.* **94**, 101915 (2009).

<sup>3</sup>J. Yoshikawa, Y. Katsuda, N. Yamada, C. Ihara, M. Masuda, and H. Sakai, *J. Am. Ceram. Soc.* **88**, 3501 (2005).

<sup>4</sup>Q. Sun, J. T. Wang, H. Wang, R. Q. Jin, D. S. Jiang, J. J. Zhu, D. G. Zhao, H. Yang, S. Q. Zhou, M. F. Wu, D. Smeets, and A. Vantomme, *J. Appl. Phys.* **104**, 043516 (2008).

<sup>5</sup>S. Raghavan, X. J. Weng, E. Dickey, and J. M. Redwing, *Appl. Phys. Lett.* **87**, 142101 (2005).

<sup>6</sup>P. Schley, C. Napierala, R. Goldhahn, G. Gobsch, J. Schormann, D. J. As, K. Lischka, M. Feneberg, K. Thonke, F. Fuchs, and F. Bechstedt, *Phys. Status Solidi C* **5**, 2342 (2008).

<sup>7</sup>I. Gorczyca, L. Dmowski, J. Plesiewicz, T. Suski, N. E. Christensen, A. Svane, C. S. Gallinat, G. Koblmüller, and J. S. Speck, *Phys. Status Solidi B* **245**, 887 (2008).

<sup>8</sup>B. A. Haskell, S. Nakamura, S. P. DenBaars, and J. S. Speck, *Phys. Status Solidi B* **244**, 2847 (2007).

<sup>9</sup>R. Armitage, J. Suda, and T. Kimoto, *Appl. Phys. Lett.* **88**, 011908 (2006).

<sup>10</sup>Y. Wu, G. Chen, H. Ye, Y. Zhu, and S.-H. Wei, *J. Appl. Phys.* **104**, 084313 (2008).

- <sup>11</sup>Q. Zhao, H. Z. Zhang, X. Y. Xu, Z. Wang, J. Xu, D. P. Yu, G. H. Li, and F. H. Su, *Appl. Phys. Lett.* **86**, 193101 (2005).
- <sup>12</sup>Y. Tokumoto, N. Shibata, T. Mizoguchi, M. Sugiyama, Y. Shimogaki, J. S. Yang, T. Yamamoto, and Y. Ikuhara, *J. Mater. Res.* **23**, 2188 (2008).
- <sup>13</sup>I. Arslan and N. D. Browning, *Phys. Rev. Lett.* **91**, 165501 (2003).
- <sup>14</sup>M. E. Hawkrige and D. Cherns, *Appl. Phys. Lett.* **87**, 221903 (2005).
- <sup>15</sup>Z. Liliental-Weber, Y. Chen, S. Ruvimov, and J. Washburn, *Phys. Rev. Lett.* **79**, 2835 (1997).
- <sup>16</sup>J. Elsner, R. Jones, M. Haugk, R. Gutierrez, T. Frauenheim, M. I. Heggie, S. Oberg, and P. R. Briddon, *Appl. Phys. Lett.* **73**, 3530 (1998).
- <sup>17</sup>J. E. Northrup, *Phys. Rev. B* **73**, 115304 (2006).
- <sup>18</sup>J. P. Perdew and Y. Wang, *Phys. Rev. B* **45**, 13244 (1992).
- <sup>19</sup>G. Kresse and J. Furthmuller, *Phys. Rev. B* **54**, 11169 (1996).
- <sup>20</sup>G. Kresse and J. Furthmuller, *Comput. Mater. Sci.* **6**, 15 (1996).
- <sup>21</sup>D. Vanderbilt, *Phys. Rev. B* **41**, 7892 (1990).
- <sup>22</sup>J. D. Pack and H. J. Monkhorst, *Phys. Rev. B* **16**, 1748 (1977).
- <sup>23</sup>A. Filippetti, V. Fiorentini, G. Cappellini, and A. Bosin, *Phys. Rev. B* **59**, 8026 (1999).
- <sup>24</sup>H. G. Ye, G. D. Chen, Y. L. Wu, Y. Z. Zhu, and S. H. Wei, *Phys. Rev. B* **78**, 193308 (2008).
- <sup>25</sup>S. H. Wei and A. Zunger, *Appl. Phys. Lett.* **69**, 2719 (1996).
- <sup>26</sup>H. G. Ye, G. D. Chen, Y. L. Wu, Y. Z. Zhu, and S. H. Wei, *Phys. Rev. B* **80**, 033301 (2009).
- <sup>27</sup>H. G. Ye, G. D. Chen, Y. Z. Zhu, and S. H. Wei, *Phys. Rev. B* **77**, 033302 (2008).